Electronic Supplementary Information

Table of Contents

General Methods	S2
Synthetic Procedures	S2
Scheme S1. Synthesis of **3** and **4**	S2
Scheme S2. Schematic representation of host-guest interactions between host **3** and guest **G1** or **G5**	S3
Synthesis of **3**	S3
Crystallographic data of **EtOAc ⊂ 3**	S3
Figure S1. ^{1}H NMR spectrum (500 MHz) of **3** in $CDCl_3$	S4
Figure S2. ^{13}C NMR spectrum (125 MHz) of **3** in $CDCl_3$	S4
Figure S3. HRMS (ESI) of **3**	S5
Synthesis of **4**	S5
Crystallographic data of **4**	S5
Figure S4. ^{1}H NMR spectrum of (500 MHz) of **4** in $CDCl_3$	S6
Figure S5. ^{13}C NMR spectrum of (125 MHz) of **4** in $CDCl_3$	S6
Figure S6. HRMS (ESI) of **4**	S7
Stoichiometry and association constant determination for the complexation of 3 and with Guest **G1** or **G5**	S7
Figure S7. 2D NOESY spectrum of the mixture of **3** and **G1** in $CDCl_3$	S8
Crystallographic data of **G1 ⊂ 3**	S9
Figure S8. Job ^{1}H NMR spectra (500 MHz, $CDCl_3$, 298 K) of **3** and **G1**	S9
Figure S9. Job plot of **3** and **G1**	S10
Figure S10. 2D NOESY spectrum of the mixture of 3 and **G2** in $CDCl_3$	S11
Figure S11. Job ^{1}H NMR spectra (500 MHz, CDCl3, 298 K) of 3 and **G2**	S12
Figure S12. Job plot of **3** and **G2**	S12
Figure S13. 2D NOESY spectrum of the mixture of 3 and **G3** in $CDCl_3$	S13
Figure S14. Job ^{1}H NMR spectra (500 MHz, CDCl3, 298 K) of 3 and **G3**	S14
Figure S15. Job plot of **3** and **G3**	S14
Figure S16. 2D NOESY spectrum of the mixture of 3 and **G4** in $CDCl_3$	S15
Figure S17. Job ^{1}H NMR spectra (500 MHz, CDCl3, 298 K) of 3 and **G4**	S16
Figure S18. Job plot of **3** and **G4**	S16
Figure S19. 2D NOESY spectrum of the mixture of **3** and **G5** in $CDCl_3$	S17

Figure S20. Job ^{1}H NMR spectra (500 MHz, $CDCl_3$, 298 K) of **3** and **G5**	S18
Figure S21. Job plot of **3** and **G5**	S18
Figure S22. ^{1}H NMR spectra of **3** upon addition of **G1**.	S19
Figure S23. ^{1}H NMR spectra of H_{OX5} peak shift of **3** upon addition of **G1**	S19
Figure S24. The non-linear curve-fitting for the complexation of **3** with **G1**	S20
Figure S25. ^{1}H NMR spectra of **3** upon addition of **G2**	S21
Figure S26. ^{1}H NMR spectra of H_{OX5} peak shift of **3** upon addition of **G2**	S21
Figure S27. The non-linear curve-fitting for the complexation of **3** with **G2**	S22
Figure S28. ^{1}H NMR spectra of **3** upon addition of **G3**	S23
Figure S29. ^{1}H NMR spectra of H_{OX5} peak shift of **3** upon addition of **G3**	S23
Figure S30. The non-linear curve-fitting for the complexation of **3** with **G3**	S24
Figure S31. ^{1}H NMR spectra of **3** upon addition of **G4**	S25
Figure S32. ^{1}H NMR spectra of H_{OX5} peak shift of **3** upon addition of **G4**	S25
Figure S33. The non-linear curve-fitting for the complexation of **3** with **G4**	S26
Figure S34. ^{1}H NMR spectra of **3** at a concentration upon addition of **G5**	S27
Figure S35. ^{1}H NMR spectra of H_{OX5} peak shift of **3** upon addition of **G5**	S27
Figure S36. The non-linear curve-fitting for the complexation of **3** with **G5**	S28
Reference	S28

Materials and Methods: Unless otherwise noted, all commercial reagents and solvents were used without purification. Flash column chromatography was performed on silica gel (200-300 mesh). ^{1}H and ^{13}C NMR spectra were recorded at a 500 MHz spectrometer with TMS as the reference, and 2D H-H NOESY was recorded at a 600 MHz spectrometer. Spectrum Mass spectra (ESI analysis) were recorded on an Esquire 6000 spectrometer (LC/MS). Single crystal X-ray diffraction data were collected on a SMART APEX 2 X-ray diffractometer equipped with a normal focus Mo-target X-ray tube (λ = 0.71073 Å). Data reduction included absorption corrections by the multi-scan method. The structures were solved by direct methods and refined by full-matrix least-squares using SHELXS-97. All non-hydrogen atoms were refined anisotropically, while hydrogen atoms were added at their geometrically ideal positions and refined isotropically.

Synthetic Procedures: Through the reaction, the quinone unit of **2** could be selectively transformed to either pillar[4]arene[1]benzoquinoneoxime (**3**) or pillar[4]arene[1]benzoquinonedioxime (**4**) in good yields.[S1]

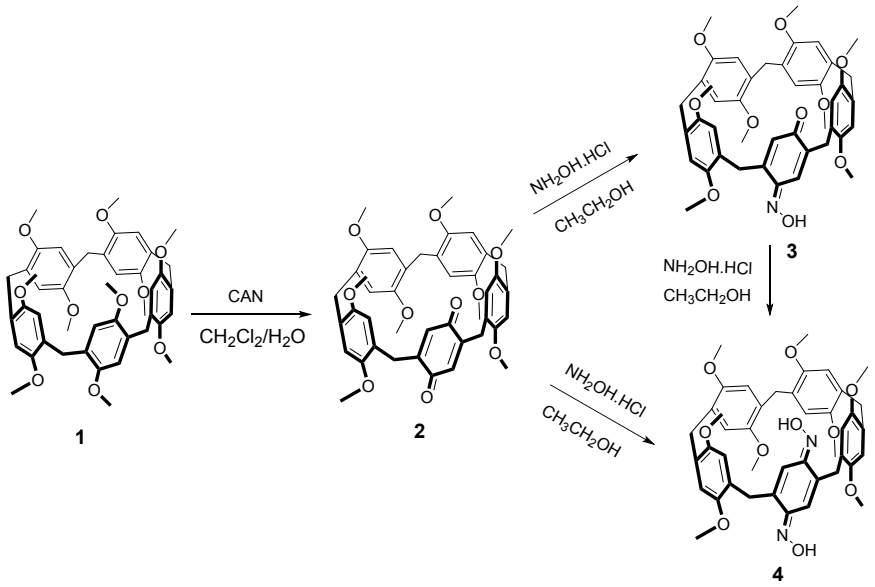

Scheme S1. Synthesis of pillar[4]arene[1]benzoquinoneoxime (**3**) or pillar[4]arene[1]benzoquinonedioxime (**4**).

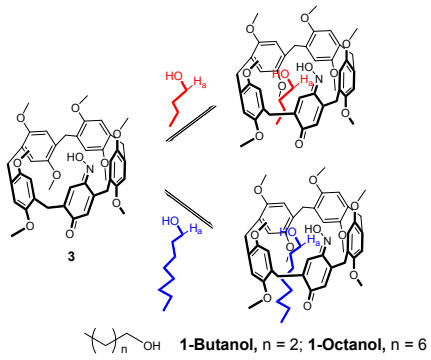

Scheme S2. Schematic representation of host-guest interactions between host **3** and guest **G1** or **G5**.

Synthesis of 3: To a solution of pillar[4]arene[1]quinone (502.6 mg, 0.70 mmol) in ethanol (25 ml, 95%) was added hydroxylammonium chloride (398.1 mg, 5.73 mmol). The mixture was heated at 78 °C for 2.5 h , then cooled to room temperature, and filtered to remove solid. The filtrate was poured into water (100 mL), and extracted with CH_2Cl_2 (3 × 20 mL). The combined organic extracts were concentrated under reduced pressure resulting in a residue which was subjected to column chromatography (petroleum ether/CH_2Cl_2 = 1:100) to afford **3** as red solid (495 mg,

96%). ^{1}H NMR (500 MHz, $CDCl_3$): δ 7.69(s, 1H), 6.85 (s, 1H), 6.84 (s, 1H), 6.82 (s, 2H), 6.80 (s, 1H), 6.78 (s, 1H), 6.77 (s, 1H), 6.68 (s, 1H), 6.46 (s, 1H), 3.63-3.81 (34H). ^{13}C NMR (125 MHz, $CDCl_3$): ^{13}C NMR (126 MHz, $CDCl_3$, 298k): δ 187.9, 151.1，151.0，150.8，150.7，150.7, 150.6, 150.3, 148.0, 141.2, 129.1, 129.1, 128.9, 128.4, 128.3, 127.9, 125.0, 124.9, 121.8, 114.4, 114.3, 114.18, 114.0, 113.9, 113.9, 113.8, 113.8, 56.0, 55.9, 55.8, 55.7, 55.7, 55.6, 52.8, 29.7, 29.52, 29.3, 28.7. HRMS (ESI): calcd for $C_{43}H_{45}NO_{10}$[M + H^+] = 736.3166, found 736.3151.

Crystallographic Data of EtOAc ⊂ 3： [$C_{47}H_{53}NO_{12}$]; *Mr* = 823.9; T = 173.15K; monoclinic; space group C2/c; a=42.729(8) b=12.651(2) c=16.865(3) Å; α =90° ; β = 95.628(8) ° ; γ =90° ; *V* = 9073(3) Å^3; Z = 8; ρcalcd = 1.206g/cm^3; μ = 0.087mm^{-1}; reflections collected 51219; independent reflections 7921; data/restraints/parameters 7921/385/552; *GOF* on F^2 1.290; *Rint* for independent data 0.1783; final R_1 = 0.1310, wR_2 = 0.3801; R indices (all data) R_1 =0.2285, wR_2 = 0.3451; largest diff. peak and hole: 1.00 and -0.72eÅ^{-3}.

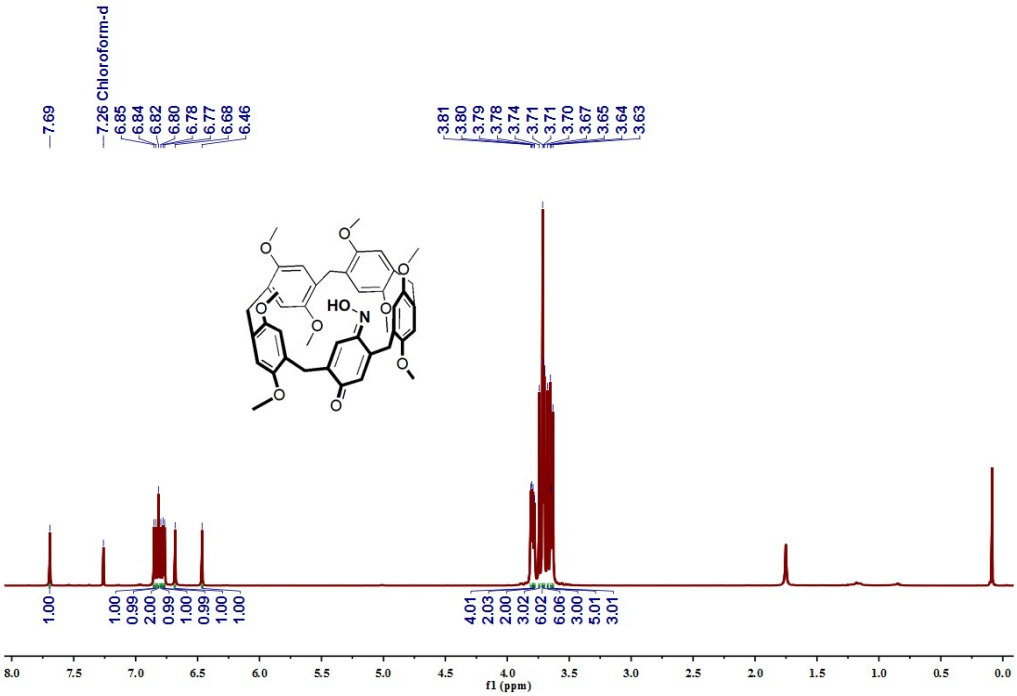

Figure S1. ^{1}H NMR spectrum (500 MHz) of **3** in $CDCl_3$.

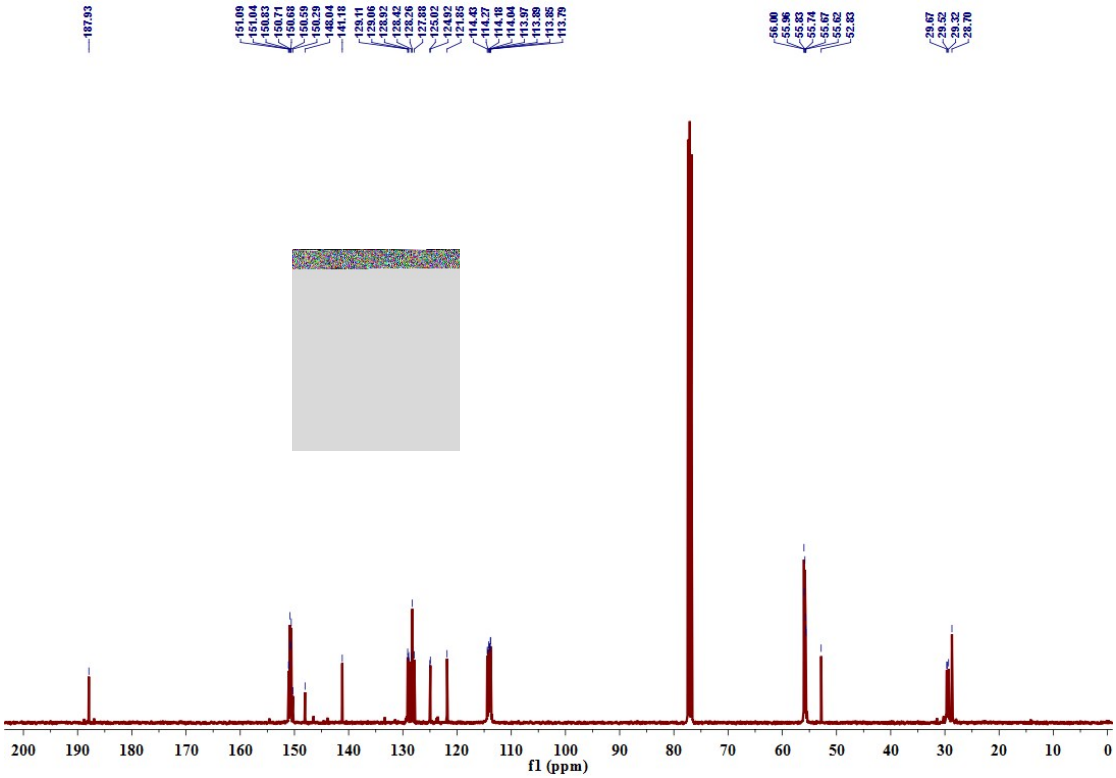

Figure S2. ^{13}C NMR spectrum (125 MHz) of **3** in $CDCl_3$.

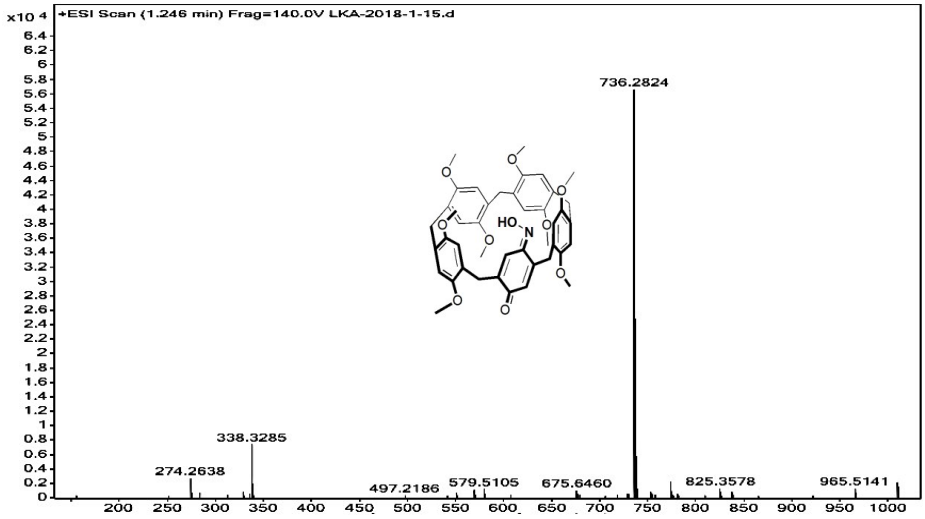

Figure S3. HRMS (ESI) of **3**： calcd for $C_{43}H_{45}NO_{10}[M + H^+]$ = 736.3166, found 736.3151

Synthesis of 4: To a solution of pillar[4]arene[1]quinone(504.9 mg,0.70 mmol) in ethanol (25 mL, 95%) was added hydroxylammonium chloride (1.70 g, 24.4 mmol). The mixture was heated at 78 °C for 48 h, then cooled to room temperature, and to remove solid. The filtrate was poured into water (100 mL), and extracted with CH_2Cl_2 (3 × 20 mL). The combined extracts were concentrated under reduced pressure

resulting in a residue which was purified by column chromatography (CH_2Cl_2/MeOH = 100:1) to afford **4** as red solid (449.6 mg, 88%). 1H NMR (500 MHz, $CDCl_3$,): δ 7.21(s, 2H), 6.80 (s, 2H), 6.76 (s, 4H), 6.73 (s, 2H), 3.62~3.80 (34H). ^{13}C NMR (125 MHz, $CDCl_3$) δ 150.7, 150.3, 150.3, 149.9, 139.8, 128.56, 128.1, 127.8, 126.2, 115.9, 113.9, 113.9, 113.7, 113.2, 113.1, 55.4, 55.2, 55.1, 54.9, 54.9, 54.1. HRMS (ESI): calcd for $C_{43}H_{46}N_2O_{10}[M + H^+]$ = 751.3225, found 751.3268.

Crystallographic Data of 4: $[C_{43}H_{46}N_2O_{10}]$; *Mr* =750.82; T = 193(2)K; Monoclinic; space group P 21/c; a= 21.701(6) b= 8.299(3) c= 23.480(7) Å; α =90° ; β = 115.537(4) ° ; γ =90° ; V = 3815(2) Å^3; Z = 4; ρcalcd = 1.307 g/cm^3; μ = 0.093 mm^{-1}; reflections collected 23542; independent reflections 7494; data/restraints/parameters 7494/ 4/512; *GOF* on F^2 1.031; *Rint* for independent data 0.1092; final R_1 = 0.0831, wR_2 = 0.2074; R indices (all data) R_1 =0.1786, wR_2 = 0.2594; largest diff. peak and hole: 1.051 and -0.366 eÅ^{-3}.

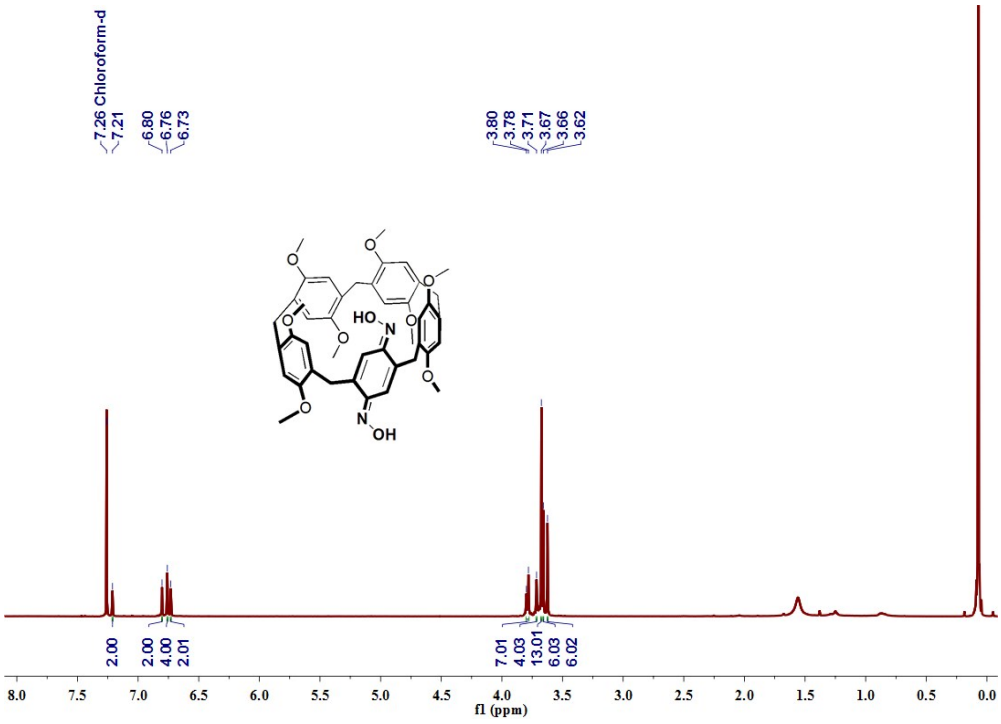

Figure S4. ^1H NMR spectrum (500 MHz) of **4** in $CDCl_3$

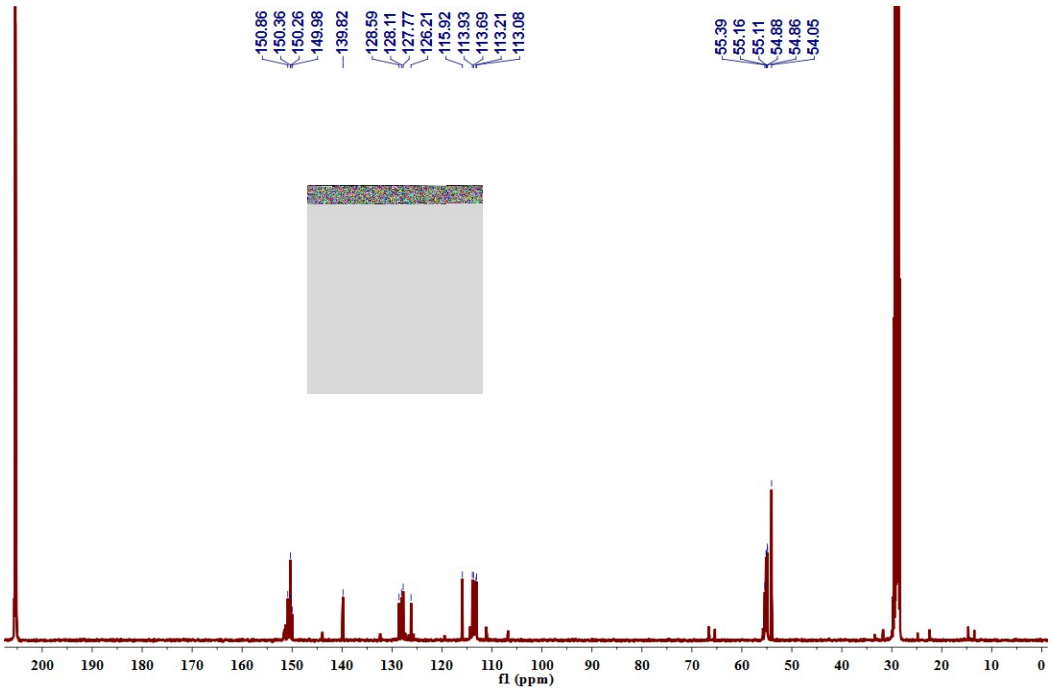

Figure S5. ^{13}C NMR spectrum (125 MHz) of **4** in $CDCl_3$.

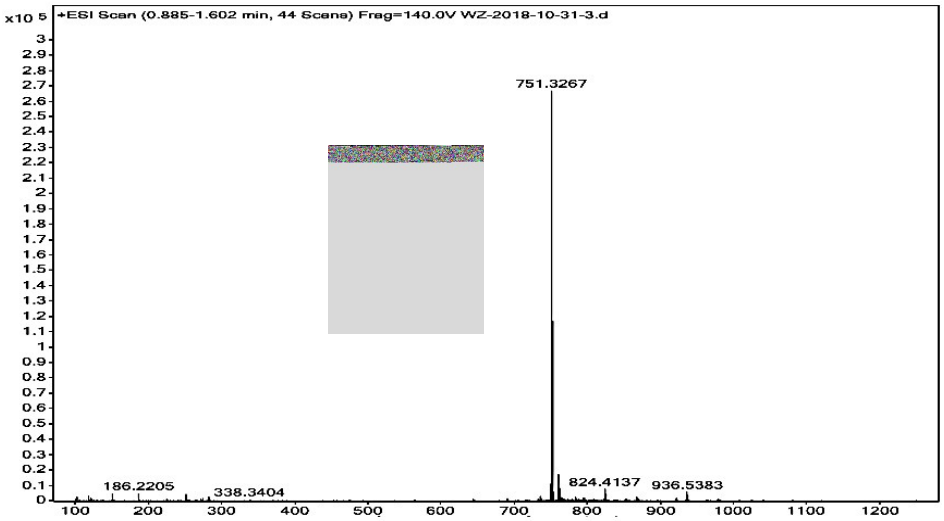

Figure S6. HRMS (ESI) of **4**: calcd for $C_{43}H_{46}N_2O_{10}[M + H^+]$ = 751.3225, found 751.3268.

Stoichiometry and association constant determination for the complexation of 3 and with guest G1 or G5.

To determine the stoichiometry and association constant between Oxime-P5 and Guest, ^1H NMR titration was carried out with solutions which had a constant concentration of **3** (5.0 mM) and varying concentrations of **G1** or **G5**. By a non-linear

curve-fitting method, the association constant between the guest and host **3** was calculated. The non-linear curve-fitting was based on the equation[2]:

$\Delta\delta = (\Delta\delta_\infty/[\mathbf{3}]_0)\ (0.5[\text{guest}]_0 + 0.5([\mathbf{3}]_0+1/K\text{a})-(0.5\ ([\text{guest}]_0^2+(2[\text{guest}]_0(1/K\text{a}-[\mathbf{3}]_0)) + (1/K\text{a} + [\mathbf{3}]_0)^2)^{0.5}))$

Where $\Delta\delta$ is the chemical shift change of H_{OX5} on Oxime-P5 at $[\text{Guest}]_0$, $\Delta\delta_\infty$ is the chemical shift change of H_{OX5} when **3** is completely complexed, $[\mathbf{3}]_0$ is the fixed initial concentration of **3**, and $[\text{Guest}]_0$ is the varying concentrations of guest (Figure S14, Figure S17).

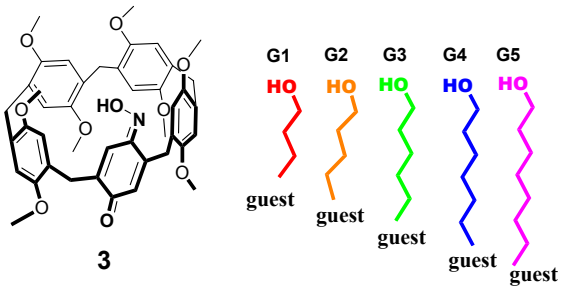

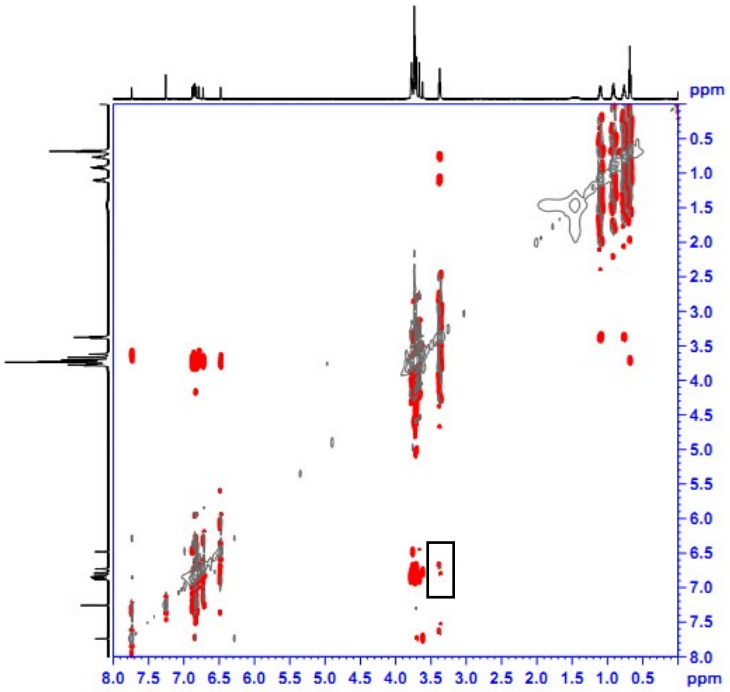

Figure S7(a). 2D NOESY spectrum of the mixture of **3** and **G1** in $CDCl_3$ (600 MHz) (The concentrations of **3** and **G1** are 41.9 mM and 83.7 mM, respectively)

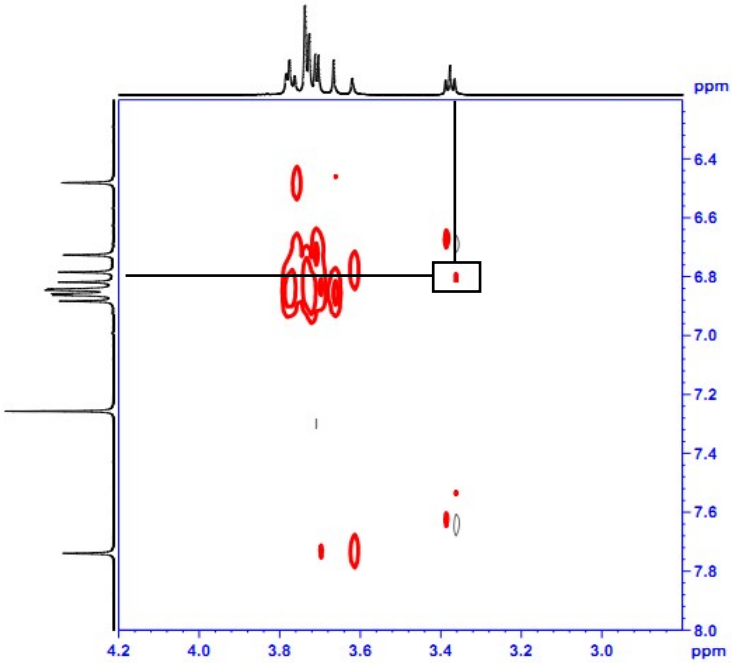

Figure S7(b). Partial 2D NOESY spectrum of the mixture of **3** and **G1** in $CDCl_3$ (600 MHz, 298 K, The concentrations of **3** and **G1** are 41.9 mM and 83.7 mM, respectively)

Crystallographic Data of G1 ⊂ 3: $[C_{47}H_{53}NO_{11}]$; *Mr* = 808.91; T = 293(2)K; monoclinic; space group $P2_1/c$; *a* = 12.1968(2); *b* = 31.9446(4); *c* = 12.4129(2)Å; α = 90° ; β = 119.137(2) ° ; γ =90° ; *V* = 4224.34(13) $Å^3$; Z = 4; ρcalcd = 1.272g/cm^3; μ = 0.736 mm^{-1}; reflections collected 110184; independent reflections 8564; data/restraints/parameters 8564/0/542; *GOF* on F^2 1.106; *Rint* for independent data 0.0586; final R_1 = 0.0633, wR_2 = 0.1400; R indices (all data) R_1 =0.0714 wR_2 = 0.1441; largest diff. peak and hole: 0.62and-0.40 e$Å^{-3}$.

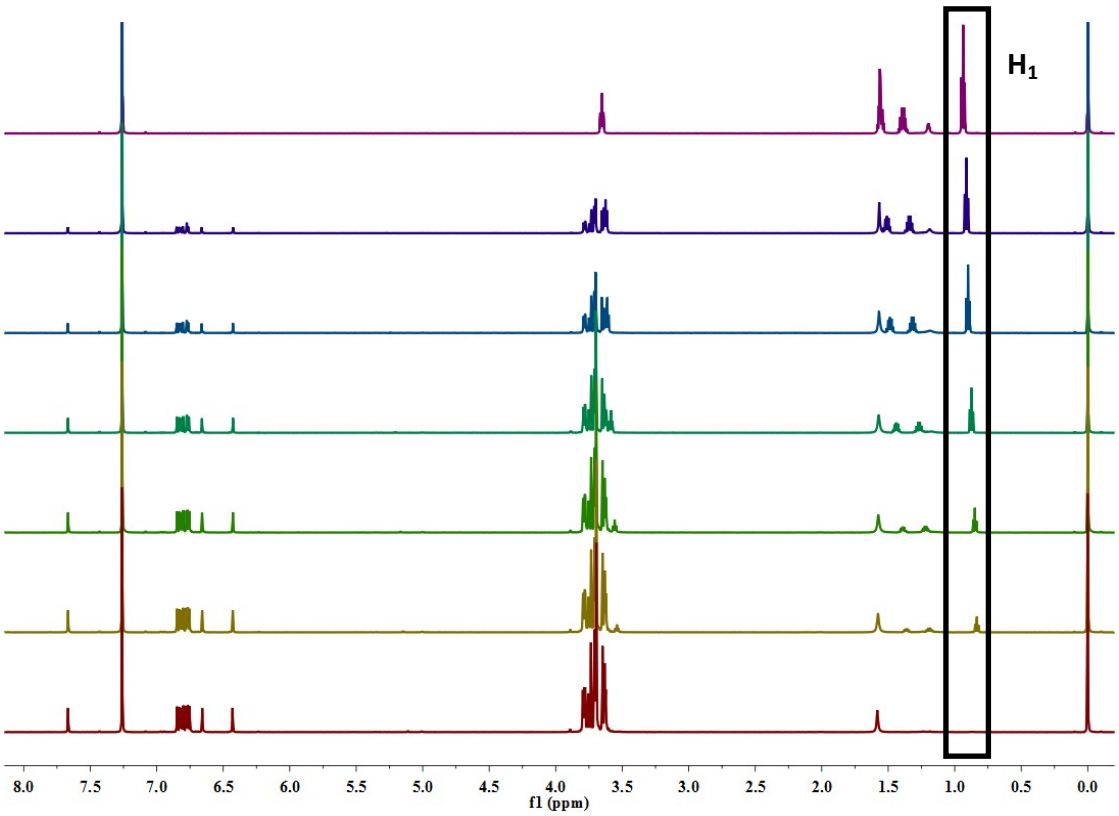

Figure S8. Job ^{1}H NMR spectra (500 MHz, $CDCl_3$, 298 K) of **3** and **G1**. From bottom to top, the concentrations of **3** were 10, 8, 7, 5, 3, 2, and 0 mM, and the concentrations of **G1** were 0, 2, 3, 5, 7, 8, and 10 mM.

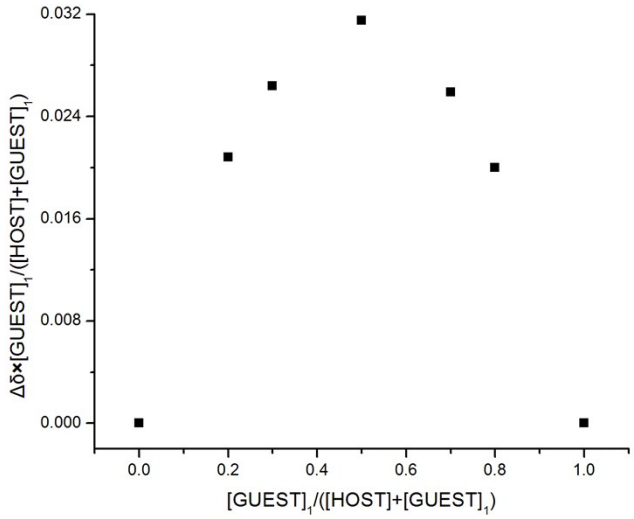

Figure S9. Job plot of **3** and **G1**. Job plot shows that the 1:1 stoichiometry of the complex between **3** and **G1** in $CDCl_3$ by plotting the Δδ of chemical shift of **G1**'s H_1 (see Figure S8) in ^{1}H NMR spectroscopy against the mole fraction of complex. ([HOST] + $[GUEST]_1$ = 10.0 mM)

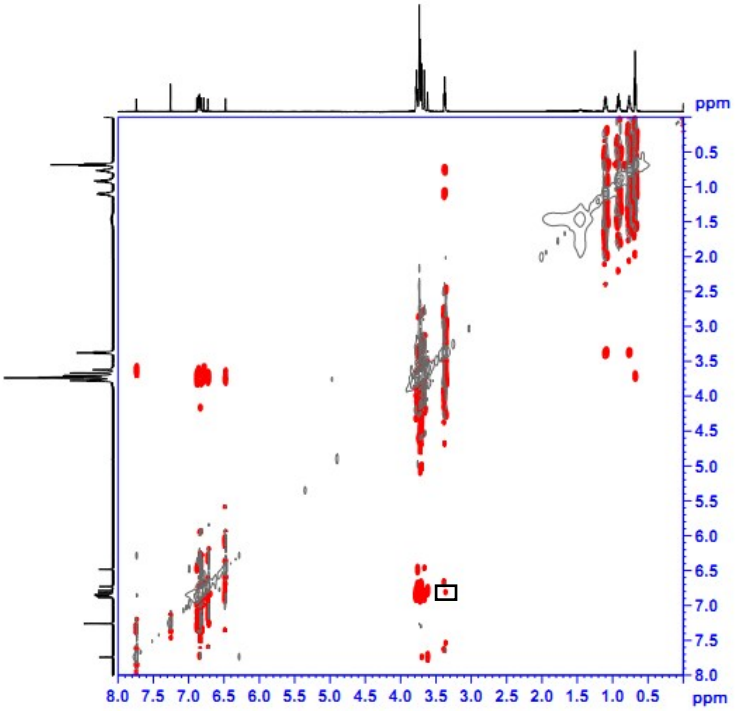

Figure S10(a). 2D NOESY spectrum of the mixture of **3** and **G2** in $CDCl_3$ (600 MHz) (The concentrations of **3** and **G2** are 41.9 mM and 83.7 mM, respectively)

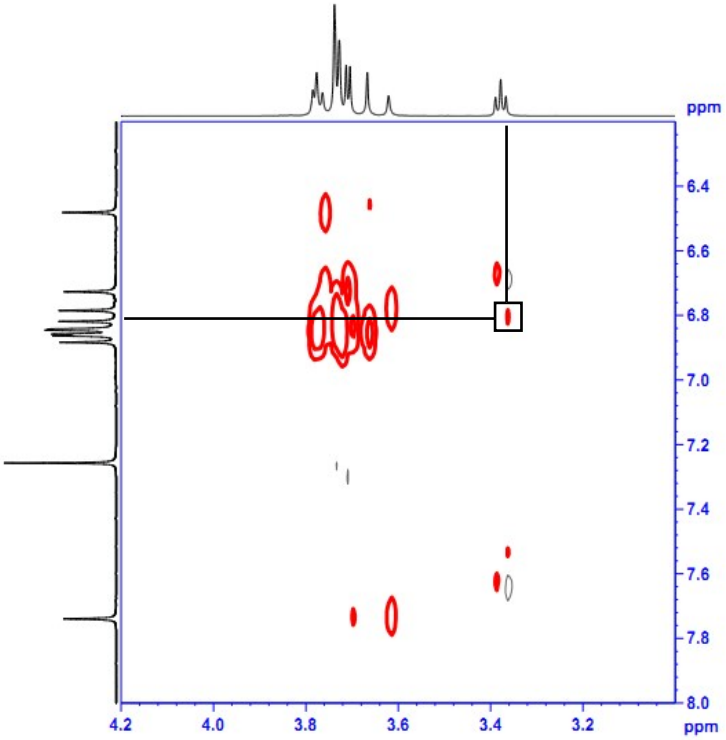

Figure S10(b). Partial 2D NOESY spectrum of the mixture of **3** and **G2** in $CDCl_3$ (600 MHz, 298 K, The concentrations of **3** and **G2** are 41.9 mM and 83.7 mM, respectively)

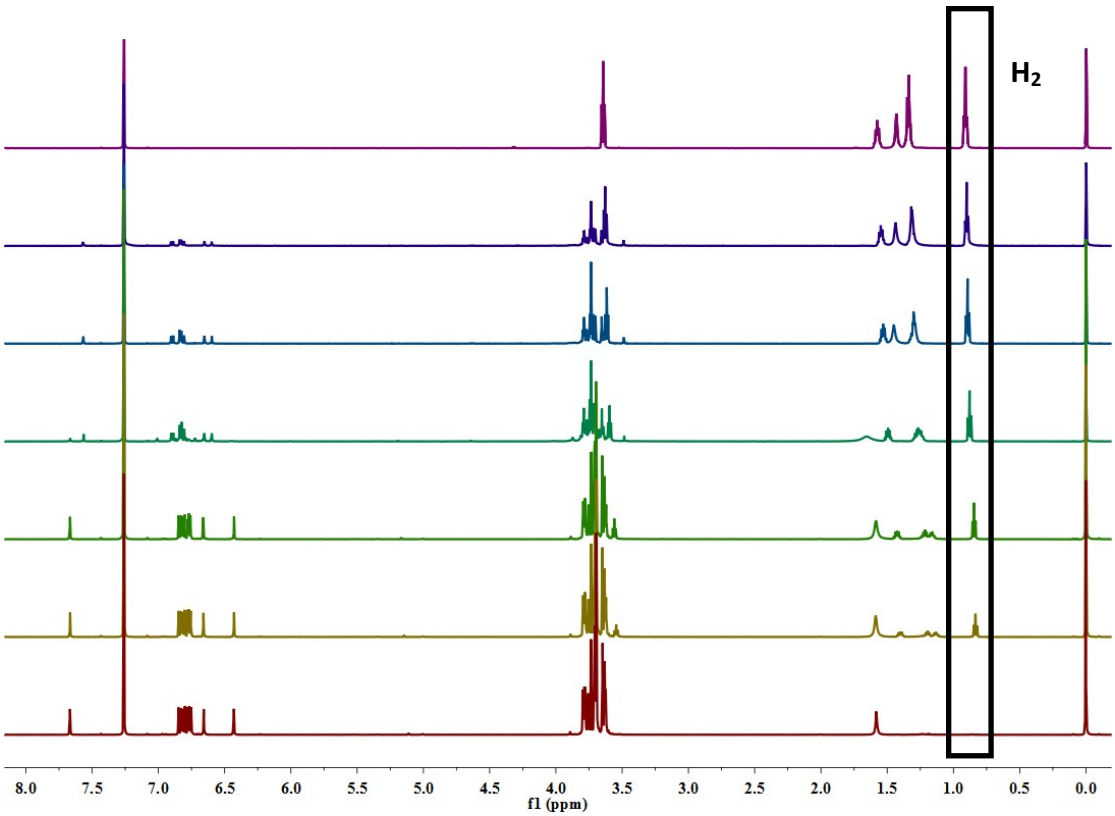

Figure S11. Job ^{1}H NMR spectra (500 MHz, $CDCl_3$, 298 K) of **3** and **G2**. From bottom to top, the concentrations of **3** were 10, 8, 7, 5, 3, 2, and 0 mM, and the concentrations of **G2** were 0, 2, 3, 5, 7, 8, and 10 mM.

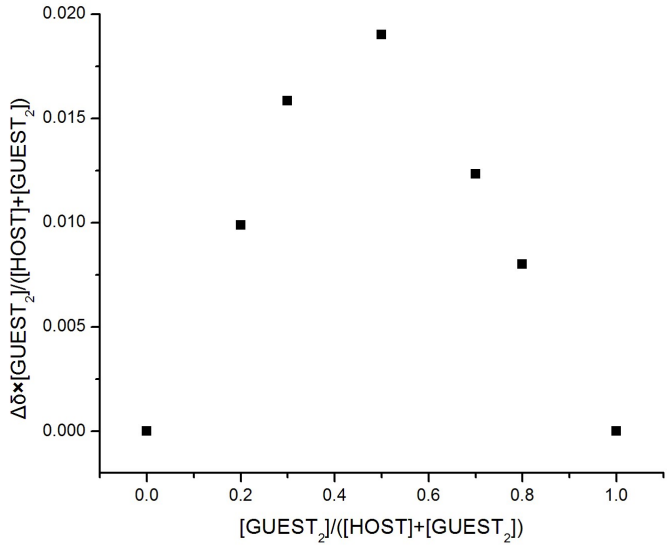

Figure S12. Job plot of **3** and **G2**. Job plot shows that the 1:1 stoichiometry of the complex between **3** and **G2** in $CDCl_3$ by plotting the Δδ of chemical shift of **G2**'s H_2 (see Figure S8) in ^{1}H NMR spectroscopy against the mole fraction of complex. ([HOST] + $[GUEST]_2$ = 10.0 mM)

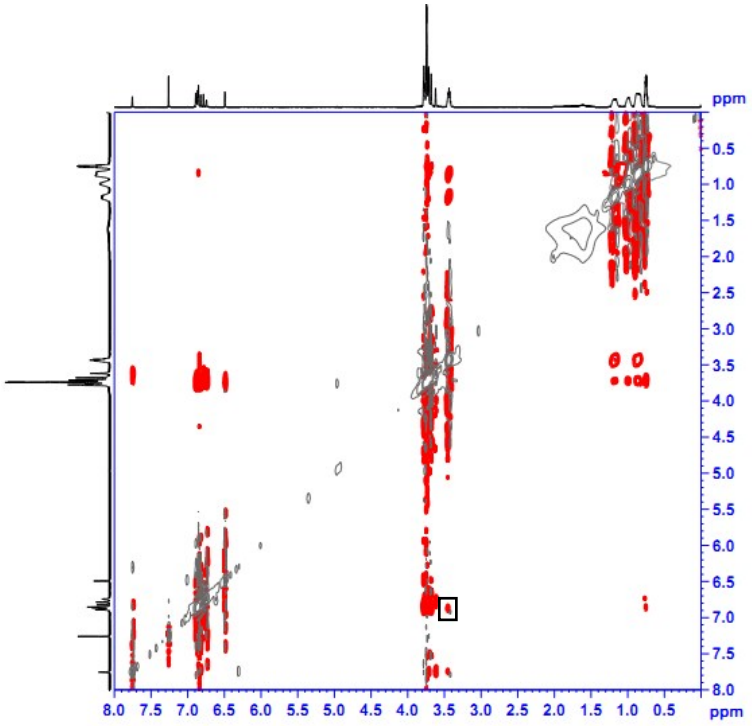

Figure S13(a). 2D NOESY spectrum of the mixture of **3** and **G3** in $CDCl_3$ (600 MHz) (The concentrations of **3** and **G3** are 41.9 mM and 83.7 mM, respectively)

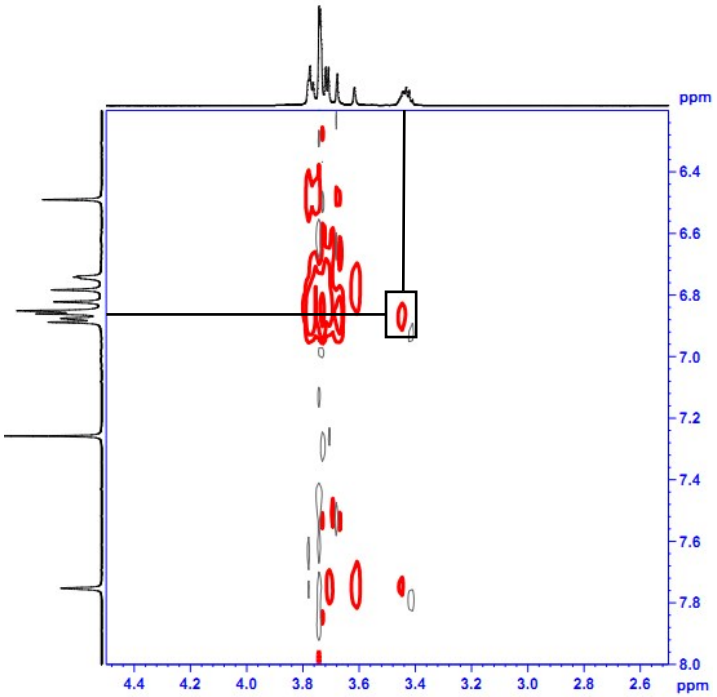

Figure S13(b). Partial 2D NOESY spectrum of the mixture of **3** and **G3** in $CDCl_3$ (600 MHz, 298 K, The concentrations of **3** and **G3** are 41.9 mM and 83.7 mM, respectively)

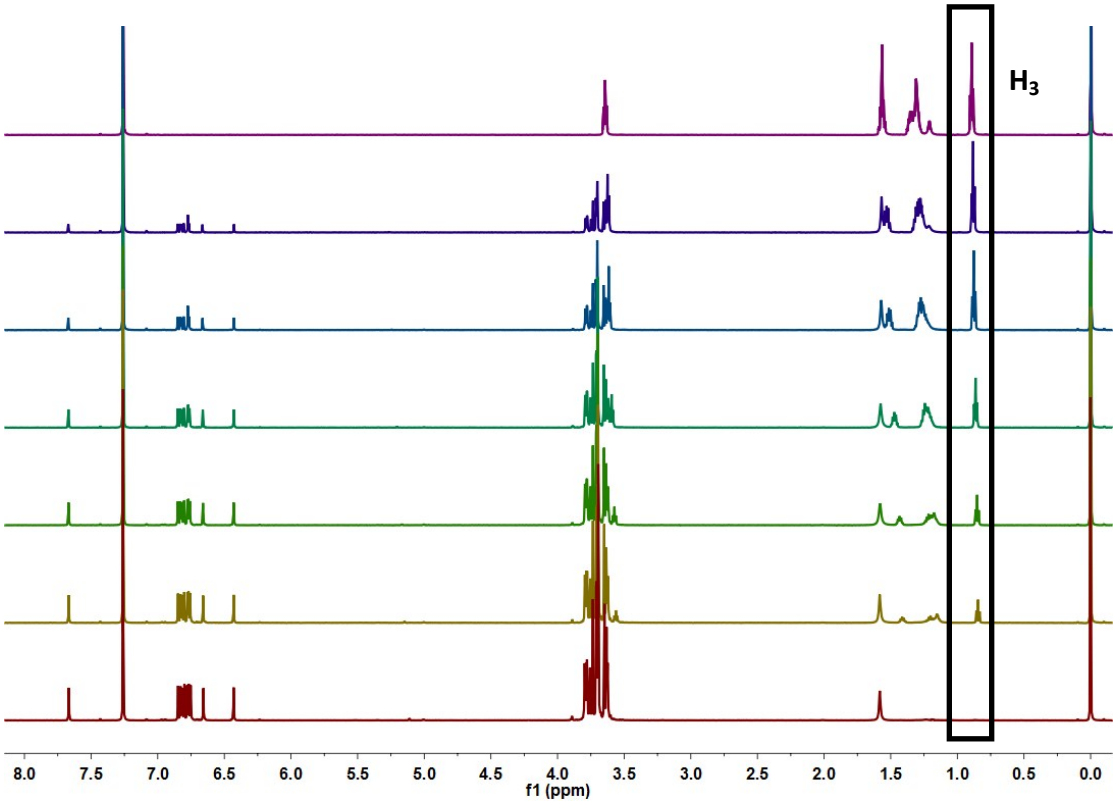

Figure S14. Job ^{1}H NMR spectra (500 MHz, $CDCl_3$, 298 K) of **3** and **G3**. From bottom to top, the concentrations of **3** were 10, 8, 7, 5, 3, 2, and 0 mM, and the concentrations of **G3** were 0, 2, 3, 5, 7, 8, and 10 mM.

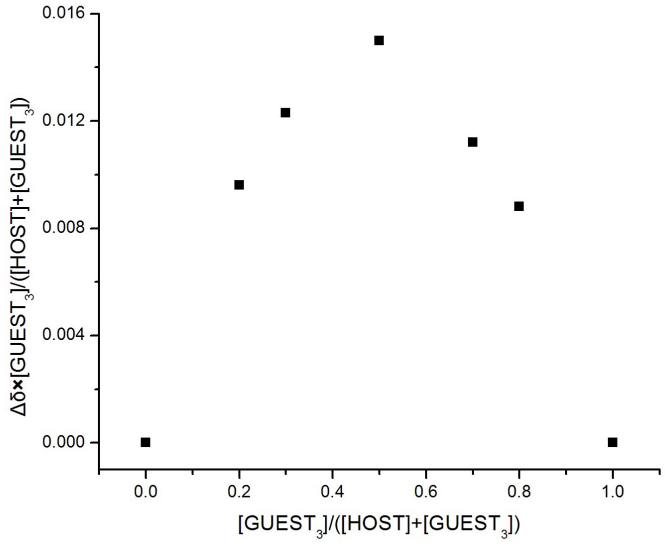

Figure S15. Job plot of **3** and **G3**. Job plot shows that the 1:1 stoichiometry of the complex between **3** and **G3** in $CDCl_3$ by plotting the Δδ of chemical shift of **G3**'s H_3 (see Figure S8) in ^{1}H NMR spectroscopy against the mole fraction of complex. ([HOST] + $[GUEST]_3$ = 10.0 mM)

Figure S16(a). 2D NOESY spectrum of the mixture of **3** and **G4** in $CDCl_3$ (600 MHz) (The concentrations of **3** and **G4** are 41.9 mM and 83.7 mM, respectively)

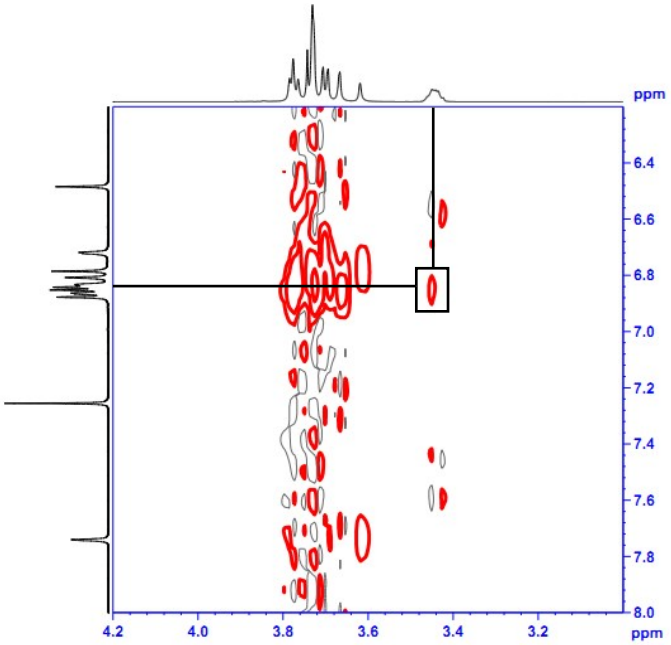

Figure S16(b). Partial 2D NOESY spectrum of the mixture of **3** and **G4** in $CDCl_3$ (600 MHz, 298 K, The concentrations of **3** and **G4** are 41.9 mM and 83.7 mM, respectively)

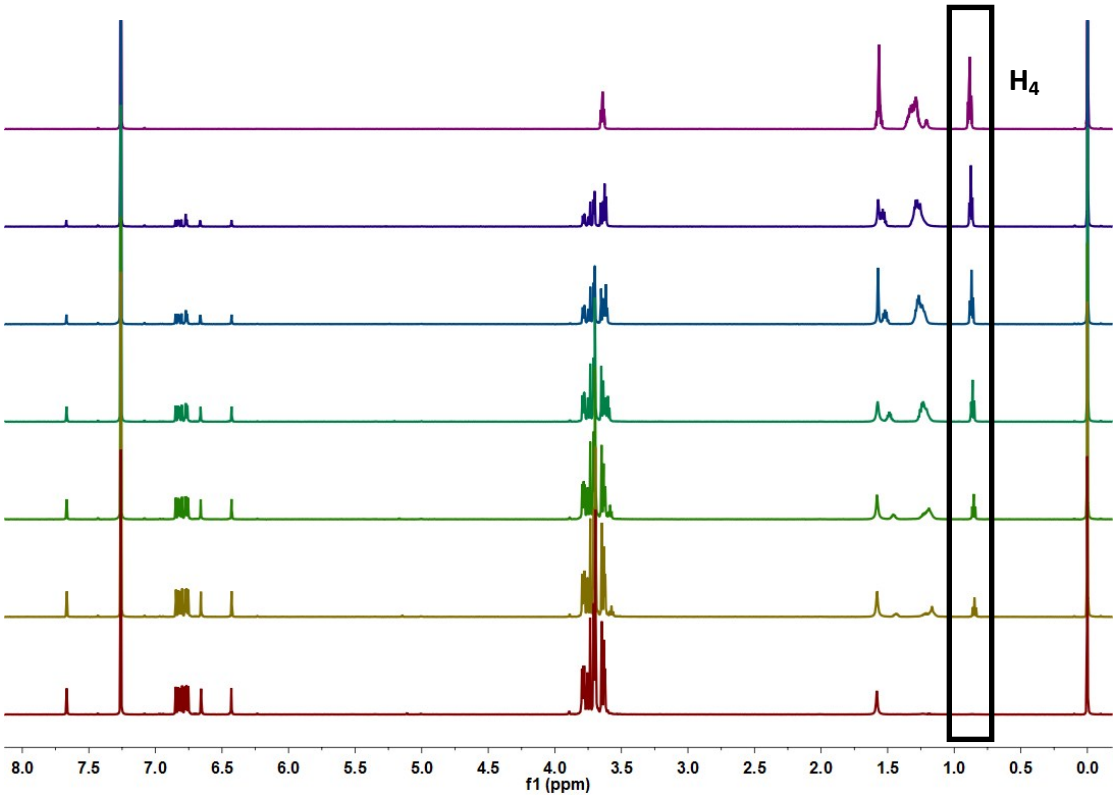

Figure S17. Job ^{1}H NMR spectra (500 MHz, $CDCl_3$, 298 K) of **3** and **G4**. From bottom to top, the concentrations of **3** were 10, 8, 7, 5, 3, 2, and 0 mM, and the concentrations of **G4** were 0, 2, 3, 5, 7, 8, and 10 mM.

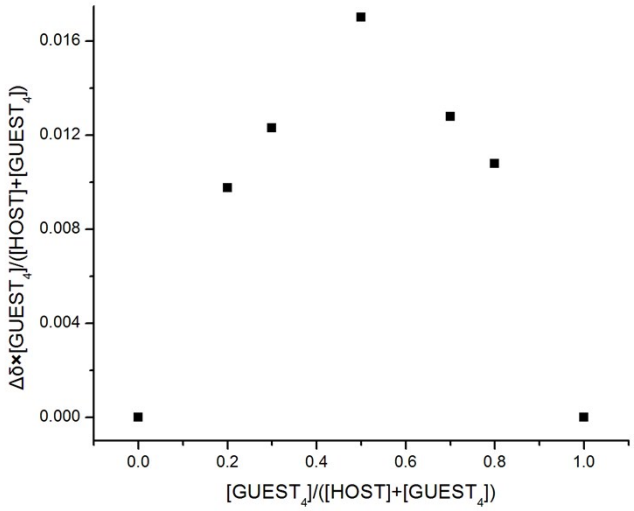

Figure S18. Job plot of **3** and **G4**. Job plot shows that the 1:1 stoichiometry of the complex between **3** and **G4** in $CDCl_3$ by plotting the Δδ of chemical shift of **G4**'s H_3 (see Figure S8) in ^{1}H NMR spectroscopy against the mole fraction of complex. ([HOST] + $[GUEST]_3$ = 10.0 mM)

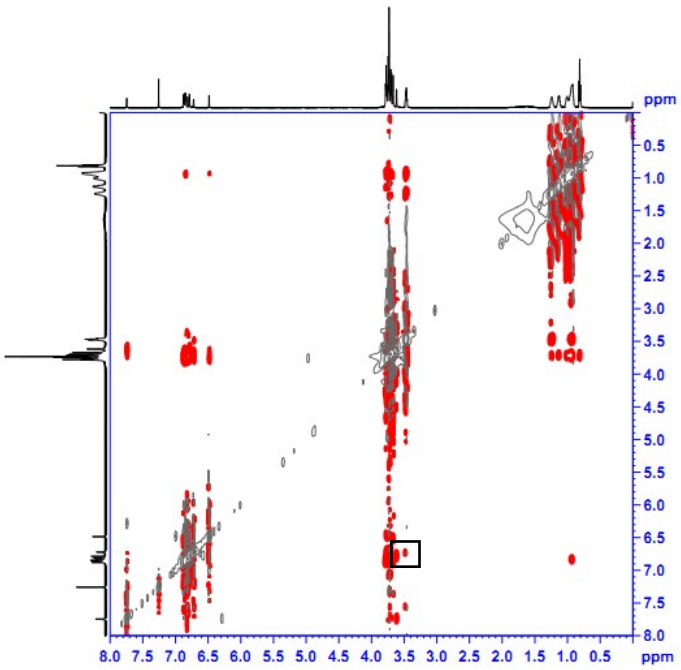

Figure S19 (a). 2D NOESY spectrum of the mixture of **3** and **G5** in $CDCl_3$ (600 MHz, 298 K, The concentrations of **3** and **G5** are 41.9 mM and 83.7 mM, respectively)

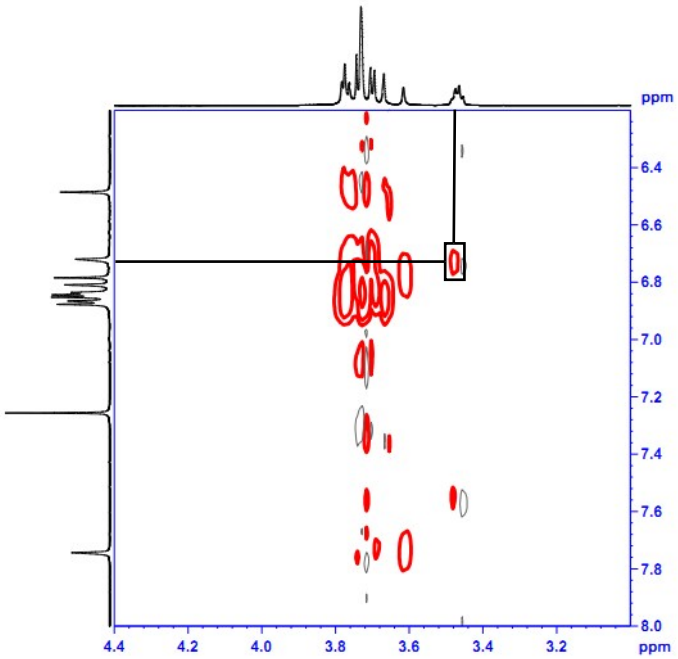

Figure S19 (b). Partial 2D NOESY spectrum of the mixture of **3** and **G5** in $CDCl_3$ (600 MHz, 298 K, The concentrations of **3** and **G5** are 41.9 mM and 83.7 mM, respectively)

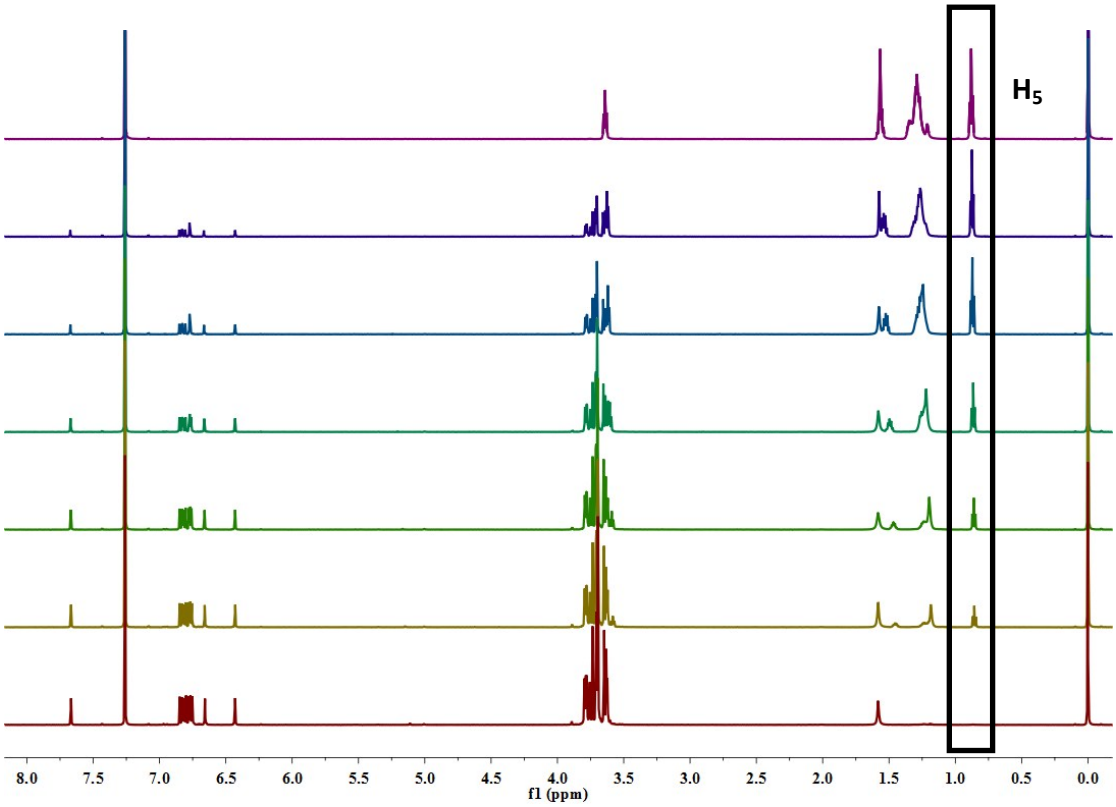

Figure S20. Job ^{1}H NMR spectra (500 MHz, $CDCl_3$, 298 K) of **3** and **G5**. From bottom to top, the concentrations of **3** were 10, 8, 7, 5, 3, 2, and 0 mM, and the concentrations of **G5** were 0, 2, 3, 5, 7, 8, and 10 mM.

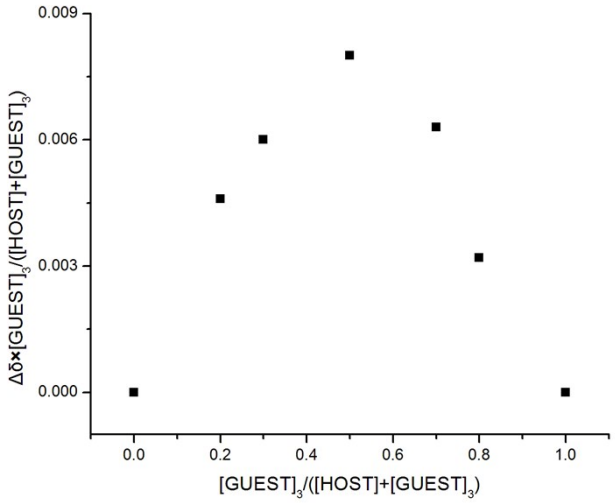

Figure S21. Job plot of **3** and **G5**. Job plot showing the 1:1 stoichiometry of the complex between **3** and **G5** in $CDCl_3$ by plotting the Δδ of chemical shift of **G5**'s H (see Figure S11) in ^{1}H NMR spectroscopy against the mole fraction of complex. ([HOST] + $[GUEST]_3$ = 10.0 mM)

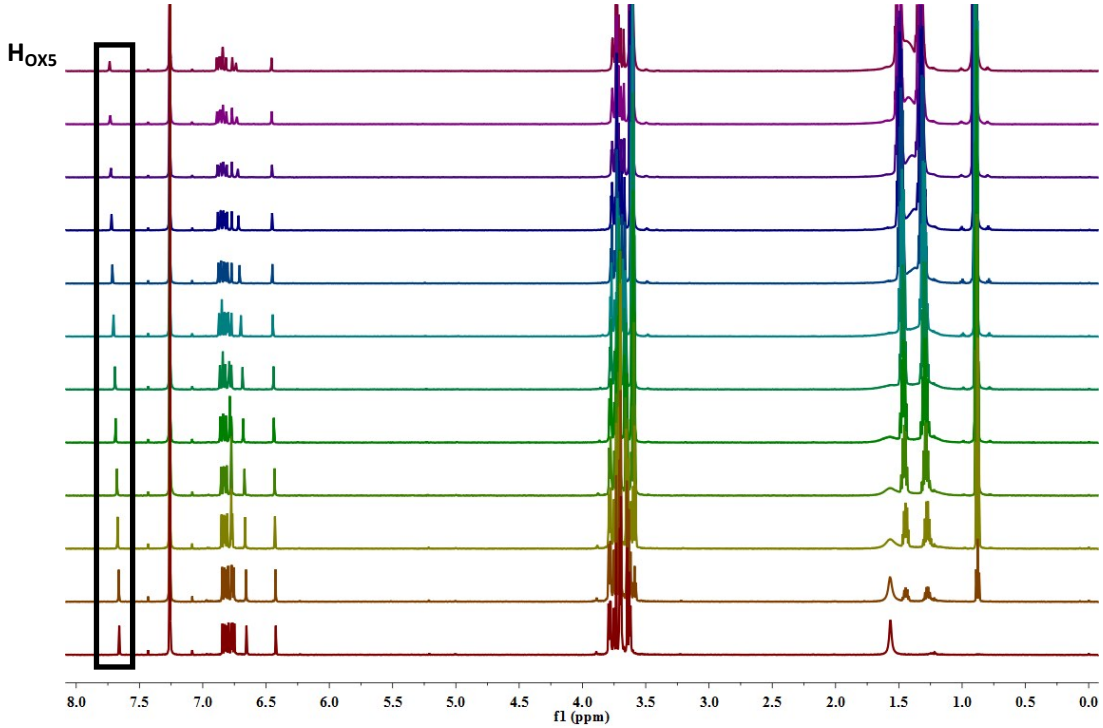

Figure S22. ^{1}H NMR spectra of **3** upon addition of **G1**. ^{1}H NMR spectra (500 MHz, $CDCl_3$, 298 K) of **3** at a concentration of 4.0 mM upon addition of **G1**. From bottom to top, the concentrations of **G1** were 0, 4, 12, 20, 32, 40, 60, 80, 100, 120, 140, and 160 mM.

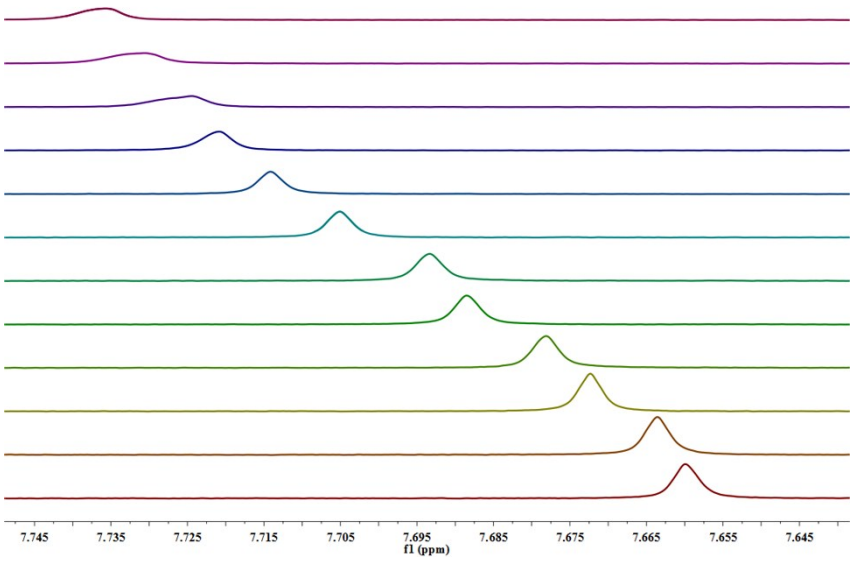

Figure S23. ^{1}H NMR spectra of H_{OX5} peak shift of **3** upon addition of **G1**. ^{1}H NMR spectra (500 MHz, $CDCl_3$, 298 K) of H_{OX5} peak shift of **3** at a concentration of 4.0 mM upon addition of **G1**. From bottom to top, the concentrations of **G1** were 0, 4, 12, 20, 32, 40, 60, 80, 100, 120, 140, and 160 mM.

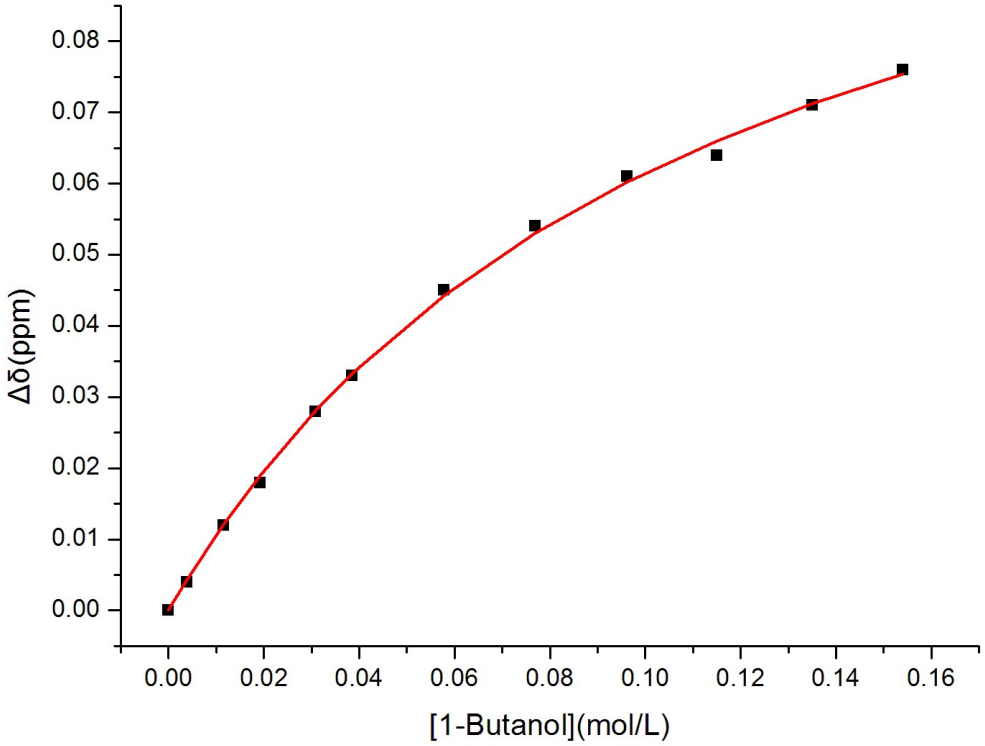

Figure S24. The non-linear curve-fitting for the complexation of **3** with **G1**. The non-linear curve-fitting (NMR titrations, Δδ of H_{OBX}) for the complexation of **3** (5.0 mM) with **G1** in $CDCl_3$ at 298 K. The concentrations of **G1** were 0, 4, 12, 20, 32, 40, 60, 80, 100, 120, 140, and 160 mM. The *K*a value for **G1** ⊂ **3** complex in $CDCl_3$ at 298 K is determined to be 9.25 ± 0.47 M^{-1} (Adj. R-Square: 0.9990).

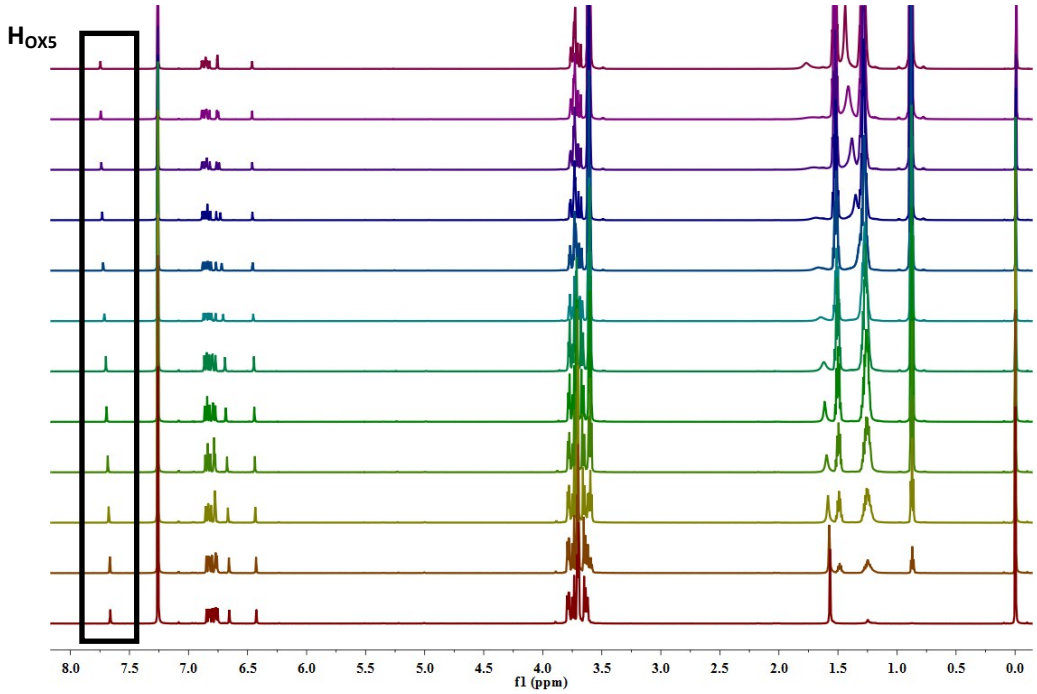

Figure S25. ^{1}H NMR spectra of **3** upon addition of **G2**. ^{1}H NMR spectra (500 MHz, $CDCl_3$, 298 K) of **3** at a concentration of 4.0 mM upon addition of **G2**. From bottom to top, the concentrations of **G2** were 0, 4, 12, 20, 32, 40, 60, 80, 100, 120, 140, and 160 mM.

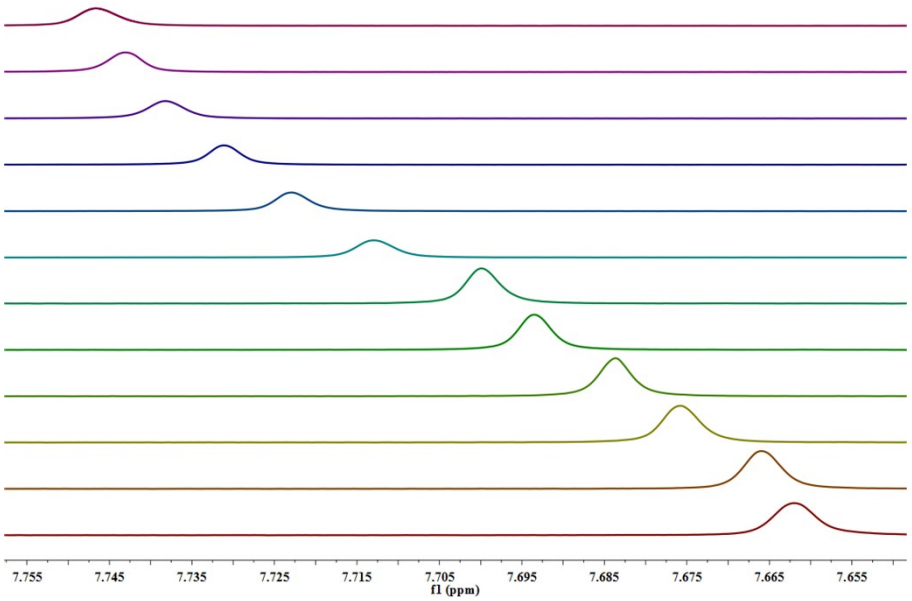

Figure S26. ^{1}H NMR spectra of H_{OX5} peak shift of **3** upon addition of **G2**. ^{1}H NMR spectra (500 MHz, $CDCl_3$, 298 K) of H_{OX5} peak shift of **3** at a concentration of 4.0 mM upon addition of **G2**. From bottom to top, the concentrations of **G2** were 0, 4, 12, 20, 32, 40, 60, 80, 100, 120, 140, and 160 mM.

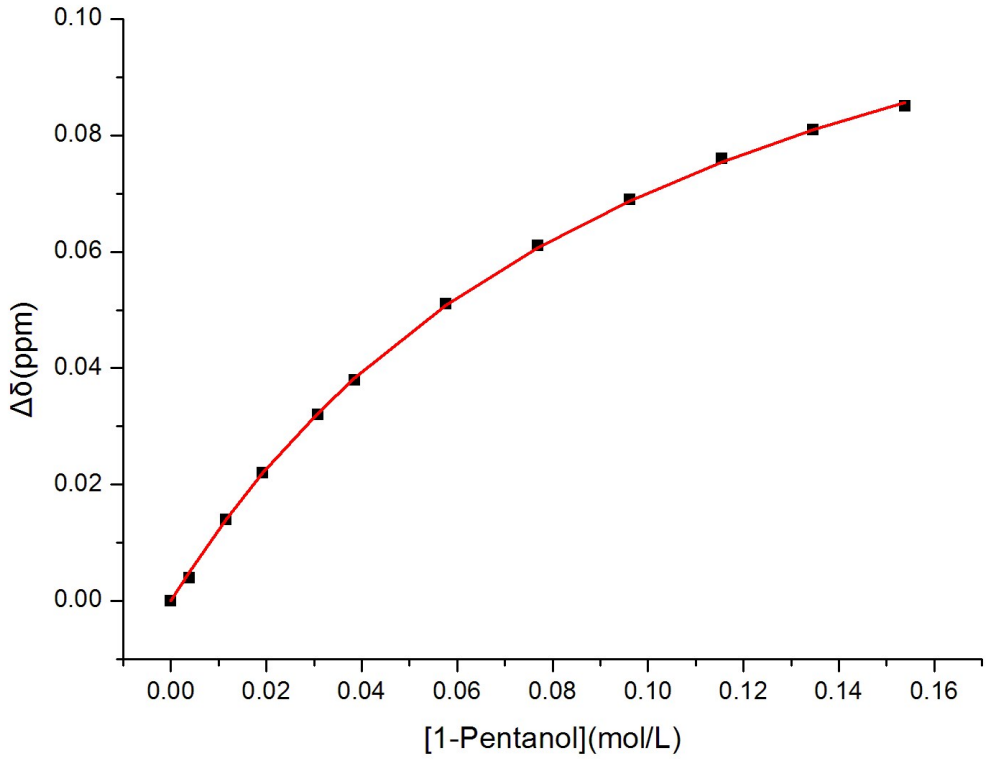

Figure S27. The non-linear curve-fitting for the complexation of **3** with **G2**. The non-linear curve-fitting (NMR titrations, Δδ of H_{OBX}) for the complexation of **3** (5.0 mM) with **G2** in $CDCl_3$ at 298 K. The concentrations of **G2** were 0, 4, 12, 20, 32, 40, 60, 80, 100, 120, 140, and 160 mM. The *K*a value for **G2** ⊂ **3** complex in $CDCl_3$ at 298 K is determined to be 9.63 ± 0.23 M^{-1} (Adj. R-Square: 0.9998).

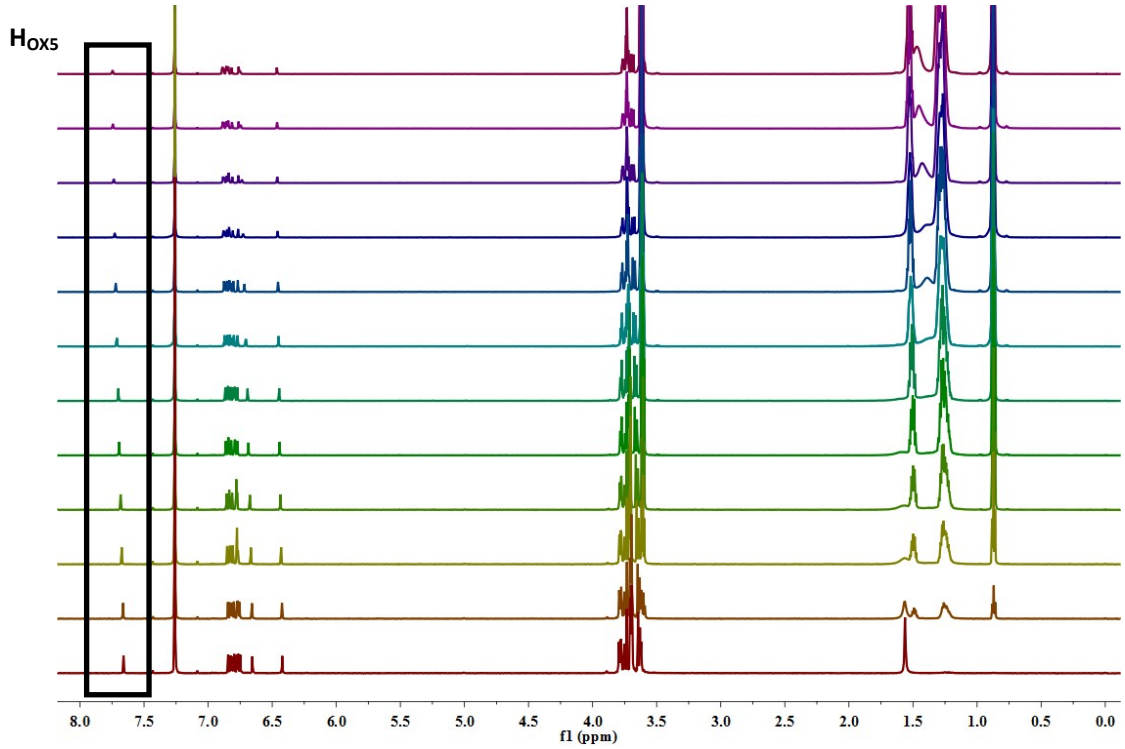

Figure S28. ^{1}H NMR spectra of **3** upon addition of **G3**. ^{1}H NMR spectra (500 MHz, $CDCl_3$, 298 K) of **3** at a concentration of 4.0 mM upon addition of **G3**. From bottom to top, the concentrations of **G3** were 0, 4, 12, 20, 32, 40, 60, 80, 100, 120, 140, and 160 mM.

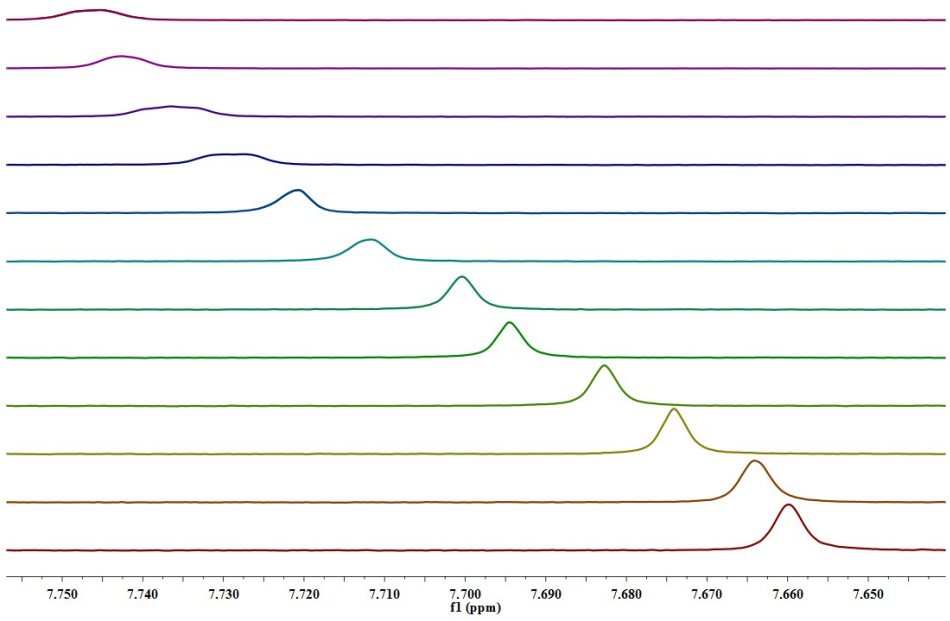

Figure S29. ^{1}H NMR spectra of H_{OX5} peak shift of **3** upon addition of **G3**. ^{1}H NMR spectra (500 MHz, $CDCl_3$, 298 K) of H_{OX5} peak shift of **3** at a concentration of 4.0 mM upon addition of **G3**. From bottom to top, the concentrations of **G3** were 0, 4, 12, 20, 32, 40, 60, 80, 100, 120, 140, and 160 mM.

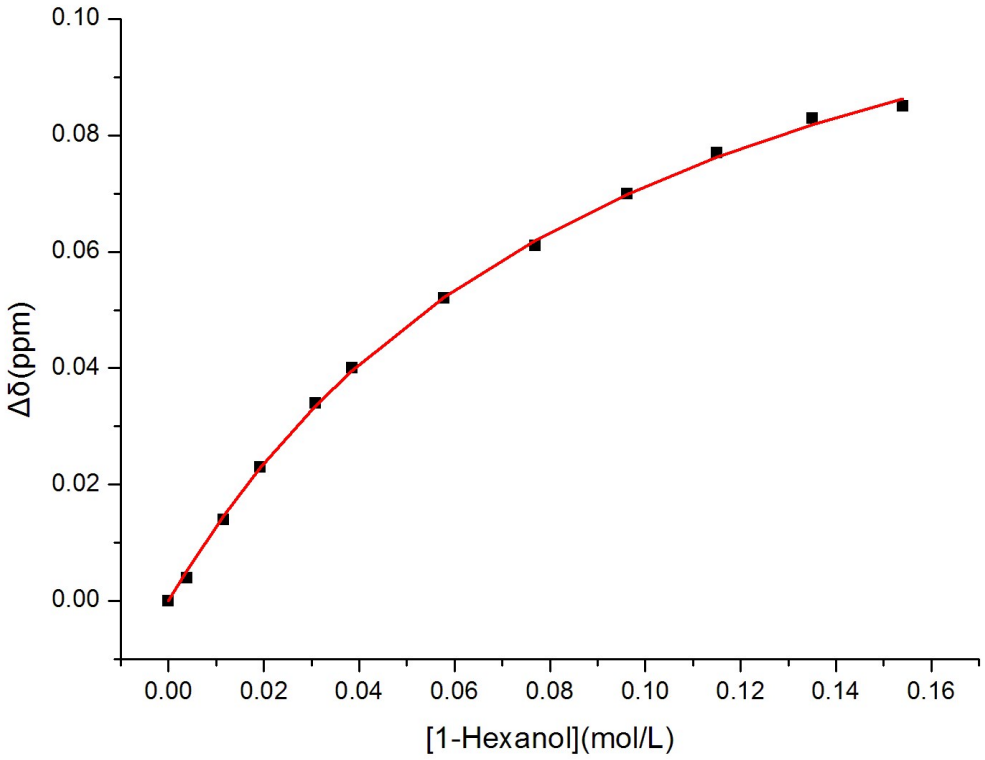

Figure S30. The non-linear curve-fitting for the complexation of **3** with **G3**. The non-linear curve-fitting (NMR titrations, Δδ of H_{OBX}) for the complexation of **3** (5.0 mM) with **G3** in $CDCl_3$ at 298 K. The concentrations of **G3** were 0, 4, 12, 20, 32, 40, 60, 80, 100, 120, 140, and 160 mM. The *K*a value for **G3** ⊂ **3** complex in $CDCl_3$ at 298 K is determined to be 10.45 ± 0.43 M^{-1} (Adj. R-Square: 0.9993).

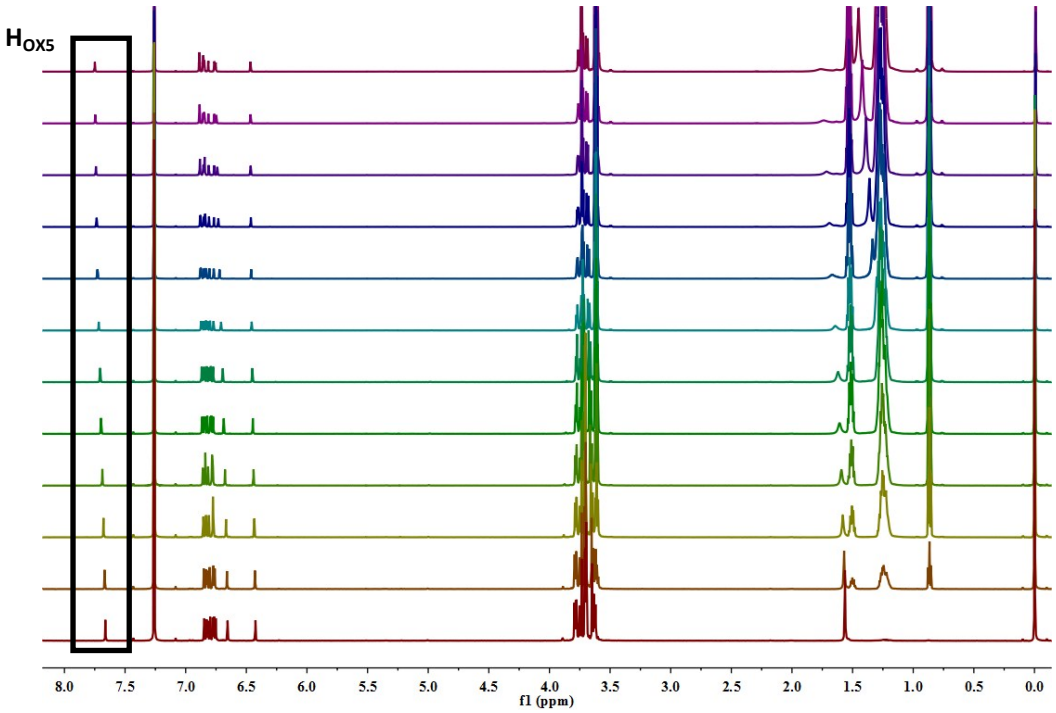

Figure S31. ^{1}H NMR spectra of **3** upon addition of **G4**. ^{1}H NMR spectra (500 MHz, $CDCl_3$, 298 K) of **3** at a concentration of 4.0 mM upon addition of **G4**. From bottom to top, the concentrations of **G4** were 0, 4, 12, 20, 32, 40, 60, 80, 100, 120, 140, and 160 mM.

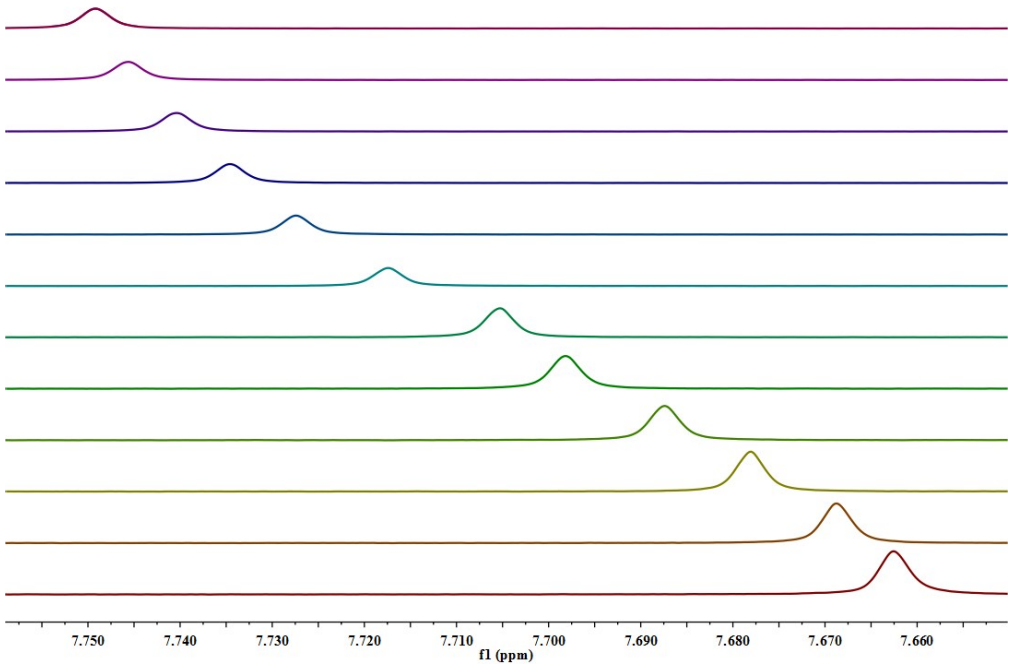

Figure S32. ^{1}H NMR spectra of H_{OX5} peak shift of **3** upon addition of **G4**. ^{1}H NMR spectra (500 MHz, $CDCl_3$, 298 K) of H_{OX5} peak shift of **3** at a concentration of 4.0 mM upon addition of **G4**. From bottom to top, the concentrations of **G4** were 0, 4, 12, 20, 32, 40, 60, 80, 100, 120, 140, and 160 mM.

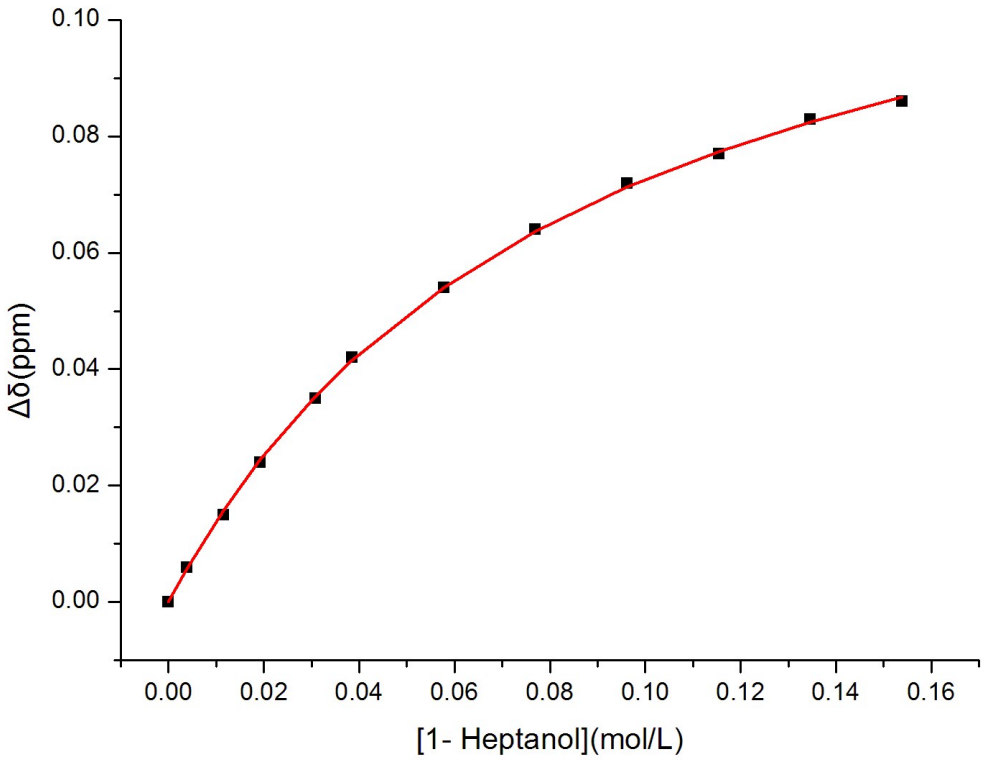

Figure S33. The non-linear curve-fitting for the complexation of **3** with **G4**. The non-linear curve-fitting (NMR titrations, Δδ of H_{OBX}) for the complexation of **3** (5.0 mM) with **G4** in $CDCl_3$ at 298 K. The concentrations of **G4** were 0, 4, 12, 20, 32, 40, 60, 80, 100, 120, 140, and 160 mM. The *K*a value for **G4** ⊂ **3** complex in $CDCl_3$ at 298 K is determined to be 11.94 ± 0.29 M^{-1} (Adj. R-Square: 0.9997).

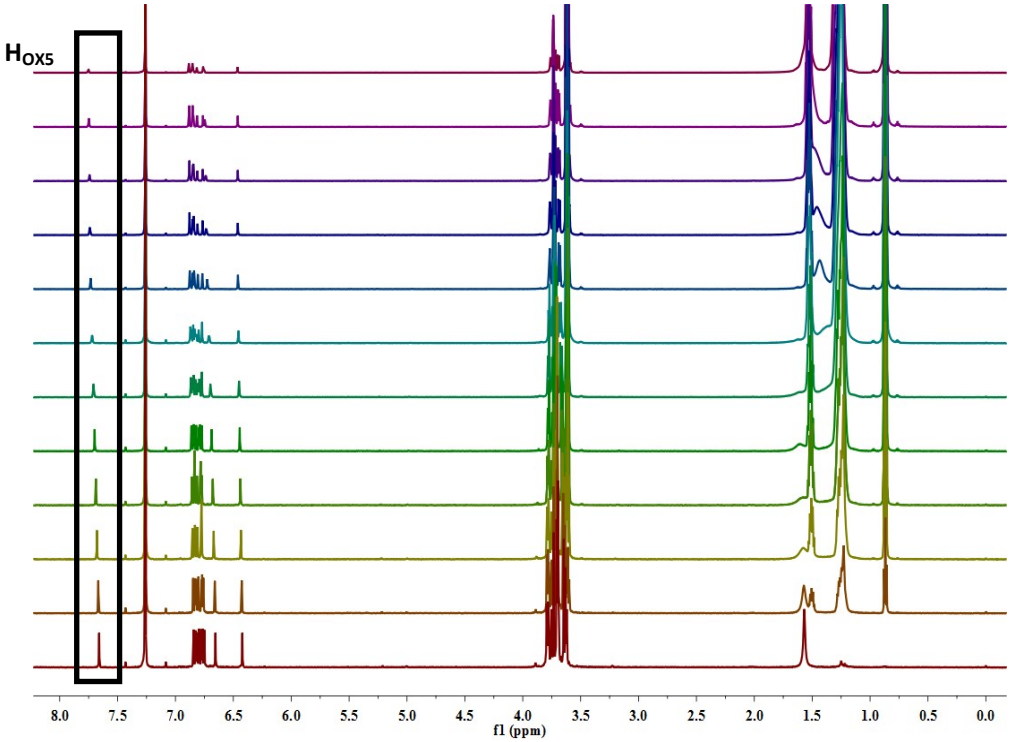

Figure S34. ^{1}H NMR spectra of **3** at a concentration upon addition of **G5**. ^{1}H NMR spectra (500 MHz, $CDCl_3$, 298 K) of **3** at a concentration of 4.0 mM upon addition of **G5**. From bottom to top, the concentrations of **G5** were 0, 4, 12, 20, 32, 40, 60, 80, 100, 120, 140, and 160 mM.

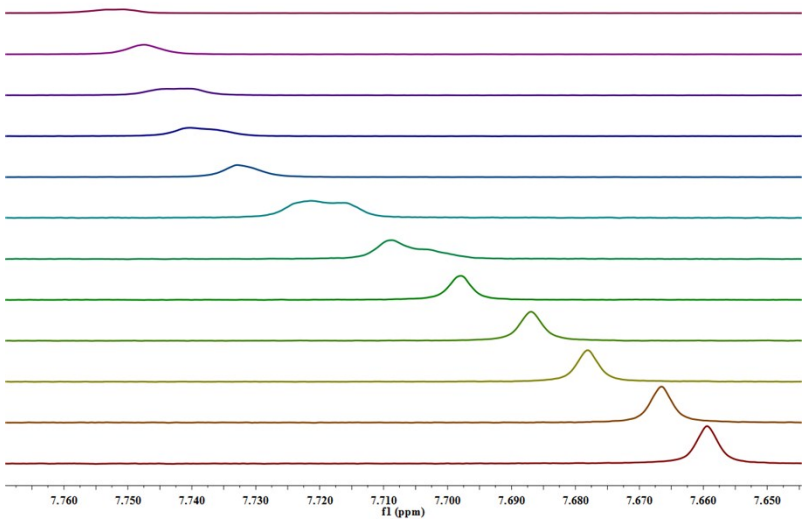

Figure S35. ^{1}H NMR spectra (500 MHz, $CDCl_3$, 298 K) of H_{OX5} peak shift of **3** at a concentration of 4.0 mM upon addition of **G5**. From bottom to top, the concentrations of **G5** were 0, 4, 12, 20, 32, 40, 60, 80, 100, 120, 140, and 160 mM.

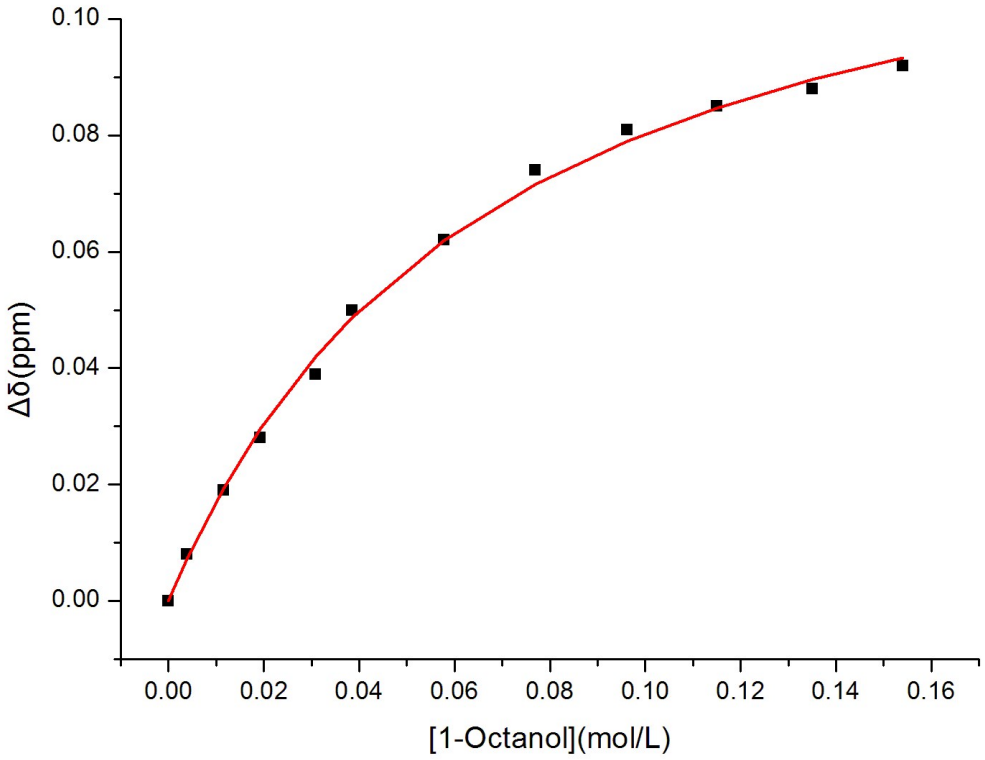

Figure S36. The non-linear curve-fitting for the complexation of **3** with **G5**. The non-linear curve-fitting (NMR titrations, Δδ of H_{OBX}) for the complexation of **3** (5.0 mM) with **G5** in $CDCl_3$ at 298 K. The concentrations of **G5** were 0, 4, 12, 20, 32, 40, 60, 80, 100, 120, 140, 160 mM, respectively. The *K*a value for **G5** ⊂ **3** complex in $CDCl_3$ at 298 K is determined to be 15.53 ±1.02 M^{-1} (Adj. R-Square: 0.9980).

References:

[1] (a) T. Ogoshi, T. Aoki, K. Kitajima, S. Fujinami, T. A. Yamagishi, Y. Nakamoto, *The J. Org. Chem.* **2011**, *76*, 328-331; (b) C. Xie, W. Hu, W. Hu, Y. A. Liu, J. Huo, J. Li, B. Jiang, K. Wen, *Chin. J. Chem.* **2015**, *33*, 379-383.

[2] (a) K. A. Connors, *Binding Constants*, Wiley: New York, **1987**; (b) R. P. Ashton, R. Ballardini, R. V. Balzani, M. Belohradsky, M. T. Gandolfi, D. Philp, L. Prodi, F. M. Raymo, M. V. Reddington, N. Spencer, J. F. Stoddart, M. Venturi, D. J. Williams, *J. Am. Chem. Soc.* **1996**, *118*, 4931; (c) Y. Inoue, K. Yamamoto, T. Wada, S. Everitt, X.-M. Gao, Z.-J. Hou, L.-H. Tong, S.-K. Jiang, H.-M. Wu, *J. Chem. Soc., Perkin Trans. 2*, **1998**, 1807.